HHS Public Access

Author manuscript

J Invest Dermatol. Author manuscript; available in PMC 2012 May 01.

Published in final edited form as:

J Invest Dermatol. 2011 November ; 131(11): 2298–2305. doi:10.1038/jid.2011.204.

Establishment of murine basal cell carcinoma allografts – a potential model for preclinical drug testing and for molecular analysis

Grace Ying Wang, **Po-Lin So**, **Lynn Wang**, **Eileen Libove**, **Joy Wang**, and **Ervin H. Epstein Jr.**

Children's Hospital Oakland Research Institute, 5700 Martin Luther King Jr. Way, Oakland, California 94609, USA

Abstract

Dysregulated hedgehog (HH) signaling has been found in numerous cancers, suggesting that therapeutic targeting of this pathway may be useful vs. a wide range of cancers. Basal cell carcinoma (BCC) is an excellent model system for studying the influence of the HH pathway on carcinogenesis because aberrant activation of HH signaling not only is crucial for the development but also for the maintenance of BCC. Genetically engineered BCC mouse models provide one important tool for the study of the biology of human BCCs and for evaluating therapeutic interventions since these mice produce multiple genetically defined tumors within a relatively short period of time. However, these models remain expensive and cumbersome to use for large-scale pre-clinical drug testing. Here we report a method for growing allografts from murine BCC tumors in NOD/SCID mice. These allografts develop faster and reproduce the histology, immunophenotypes and response to at least one anti-BCC drug of the parental autochthonous tumors from which they arise. Therefore, the allograft model provides a practical model for (i) studying BCC carcinogenesis and (ii) initial pre-clinical screening for anti-HH pathway and other anti-BCC drugs.

Keywords

Basal cell carcinoma; allograft; mouse model

INTRODUCTION

Basal cell carcinoma (BCC) is the most prevalent cancer in the Western world, and its incidence is increasing worldwide. Most BCCs occur sporadically but patients with the basal cell nevus (Gorlin) syndrome (BCNS, OMIM #109400), are predisposed to developing large numbers of BCCs. Mutational activation of hedgehog (HH) signaling underlies both familial

Correspondence: Ervin H. Epstein, Jr. Children's Hospital Oakland Research Institute, 5700 Martin Luther King Jr. Way, Oakland, California 94609, USA. eepstein@chori.org; Phone: 510 450 5688; Fax: 510 597 7096.

CONFLICT OF INTEREST

The authors state no conflict of interest.

and sporadic BCCs. Approximately 90% of sporadic BCCs have loss-of-function mutations in *Patched 1 (PTCH1)* and others have activating mutations in the downstream *Smoothened* (*SMO*) gene (Epstein 2008). Based on this knowledge, several murine models have been developed in which the transgenic over-expression of activators or the deletion of repressors drives skin HH signaling. We have focused on the Ptch1 heterozygous (Ptch1+/−) mouse, in which ionizing or ultraviolet radiation produces multiple BCCs (Aszterbaum et al 1999), thus mimicking BCNS patients. However, this and other autochthonous tumor models remain cumbersome and expensive for initial in vivo pre-clinical testing of anti-BCC agents. By contrast, the use of tumor allograft models has been well established for many cancers, providing many advantages for preclinical screening: shorter tumor latency, a more predictable growth rate, and the production of essentially identical tumor replicates.

Attempts to grow *human* BCCs as mouse xenografts met with little success. Studies relying on nude mice yielded low percentages of tumor uptake and slow growth rates (Grimwood et al 1985, Pawlowski & Haberman 1979). In some cases, various degrees of differentiation occurred in tumor transplants (Loning & Mackenzie 1986, Stamp et al 1988). Recent studies using more severely immunocompromised models, i.e. beige-nude or SCID-beige mice, moderately improved the implantation efficiency (Carlson et al 2002, Grimwood & Tharp 1991). However, it has not been determined whether these xenografts resemble their parental BCC tumors in their histology, immunophenotypes, and response to drug treatment.

Here we show that *murine* BCC cells transplanted with Matrigel into NOD/SCID mice, a newer immunocompromised mouse model, produce allografts that histologically and immunophenotypically reproduce the parental autochthonous tumors from which they were derived. To our knowledge, such BCC allografts have not been reported previously. Furthermore, we demonstrate that allografts respond to tazarotene treatment in a manner similar to that of autochtonous tumors, indicating that the allografts may indeed be a useful anti-BCC agent evaluation system.

RESULTS

Establishment of BCC allografts

To establish murine BCC allografts, we harvested visible BCC tumors from ionizing radiation treated Ptch1+/− mice in which p53 had been deleted specifically from K14-expressing keratinocytes. We selected primary tumors with sizes ranging from 100 to 400 mm^3 with no obvious ulceration or necrosis, as we found that both factors reduce the recovery of viable cells (data not shown), prepared single cell suspensions from the tumors with a typical yield of $0.5–5\times10^7$ cells per tumor, and injected NOD/SCID mice with 10^3 to 2×10^6 cells per injection site subcutaneously. The average frequency of tumor initiating cells (TICs) was 1:5.2 $\times10^5$ (L-calc, StemCell Technologies Inc.). With our optimized protocol, in particular using collagenase to free tumor cells and injecting Matrigel with the cells, we achieved 100% allograft growth when we injected $\geq 10^6$ cells. Injection of more than 10^6 cells expedited the appearance of detectable tumors (3 weeks for 2×10^6 vs. 5 weeks for 10^6) and enhanced the growth rate of tumors once they became palpable (Figure 1b, TTEST, paired, $p<0.001$). We serially transplanted these primary allografts twice before ending the experiments. Besides having a much shorter tumor latency (3–5 weeks vs. 5

months), the allografts grew significantly faster than did autochthonous tumors (Figure 2a). In addition, the growth rate continued to increase with further transplantation, i.e. tertiary transplants > secondary transplants > first transplants > primary tumors (Figure 2b). Consistent with the augmented growth, allografts had a higher percentage of Ki67-postive cells than did the primary tumors (Figure 2c). The above data suggest that the number of tumor initiating cells (TICs) may be enriched through in vivo passaging of BCCs in NOD/SCID mice. At euthanasia we saw no gross abnormality of lung, liver, or lymph nodes, suggesting that, like autochthonous BCCs, BCC allografts did not metastasize.

We were also able to grow BSZ cells, the one of our three immortalized murine BCC cell lines (Aszterbaum et al 1999, So et al 2006) tested, as allografts. We propagated the BSZ cells as tumors in vivo for 5 passages before ending the experiment and found results similar to those with allografts derived from primary tumors, i.e. short tumor latency, increased growth rate, and lack of metastasis (data not shown), despite the cell line having been passaged previously for a decade.

Comparison of BCC allografts with the primary tumors from which they were established

We have found that visible BCCs developing from ionizing radiation-treated Ptch1+/− mice with K14-specific deletion of p53 are of two histological subtypes: Type I BCCs with branching and radiating tumor cells reminiscent of follicular differentiation, some of which contain smooth muscle actin (SMA), and Type II BCCs with basaloid cells arrayed in nests not resembling follicular differentiation and lacking expression of tumor cell SMA (Mancuso et al 2006, Wang et al 2011). Interestingly, we found that the allografts established from tumors of each subtype retained the type I or type II classification of the tumors from which they arose, indicating that the histologic subtype is an intrinsic characteristic of these cells (Figure 3).

Next, we compared the immunohistologic (IHC) phenotypes of the allografts with their parental tumors, assaying for the basal keratinocyte marker keratin 14 (K14), proliferation (Ki67), vasculature (CD31), stromal distribution (collagen IV), and HH signaling activity (Gli1). As shown in Figure 4, both the allografts and their parental counterparts expressed K14 robustly, consistent with their keratinocyte cell of origin. It has been reported that orthotopic ductal pancreatic cancer autografts and xenografts have greater vascularity and a shorter distance between blood vessels and tumor cells than do the autochthonous tumors from which they are derived (Olive et al 2009). However, our BCC allografts had a density and distribution of CD31+ blood vessels and stroma surrounding tumors histologically similar to that of their primary counterparts. To identify the origin of the stromal cells we probed allografts derived from primary tumors of male mice grown in female NOD/SCID mice using a Y-chromosome specific probe. Stromal cells were identified by lack of K14 staining. As shown in Figure 5, the allografts and primary tumors had a similar percentage of Y-chromosome labeled stromal cells, indicating that some, if not all, of the stromal cells in direct allografts were from the original tumors.

Murine BCCs driven by transgenic Gli2 expression need continuous HH signaling to maintain tumor growth (Hutchin et al 2005). Therefore we next measured mRNA levels of Gli1, a well-established read-out of HH signaling, in autochthonous tumors, direct allografts,

and in the established BCC cell line (BSZ) grown both in vitro and in allografts (Figure 6). Primary, autochthonous BCCs have the highest levels of Gli1 mRNA expression, and the levels are much (approximately 22 fold) lower in the BSZ cells grown in vitro. However, growth of the autochthonous tumor cells as allografts reduced their Gli1 mRNA levels and growth of the BSZ cells as allografts elevated their Gli1 mRNA levels so that the Gli1 levels did not differ significantly between allografts grown from the two sources.

Tazarotene inhibits BCC allograft growth

Since the BCC allografts histopathologically reproduce their primary tumors and grow significantly faster with shorter tumor latency than the autochthonous tumors, they potentially provide a model for screening anti-BCC drugs more rapidly. As a proof of principle, we tested the effects on allografts of oral tazarotene, whose topical applications strongly inhibit autochthonous Ptch1+/− murine BCC carcinogenesis (So et al 2008, So et al 2004). For this we pooled 3 BCC tumors from IR-treated Ptch1+/− K14CreER2 p53fl/fl mice, injected single cell suspensions into 2 sites per NOD/SCID mouse, and divided the NOD/SCID mice randomly into 3 groups: a prevention group receiving tazarotene starting on the same day as the tumor cells were injected; a treatment group starting tazarotene when allograft tumors became palpable; and a control group injected only with tumor cells. As shown in Figure 7, six weeks of oral tazarotene completely blocked the appearance of palpable tumors in the prevention group and markedly inhibited the growth of palpable tumors in the treatment group (Figure 7, p=0.04 and 0.03). By the end of the initial 6-week administration of 10 mg/kg at 5 days per week, body weights had decreased significantly in the prevention and treatment groups but not in the control group, indicating that this dose was toxic. Therefore, we reduced the dose to 2 mg/kg and treated the mice for another 5 weeks. At this lower dose, the drug-treated mice regained their body weights to levels similar to those of the control mice, while the tumor volumes of the treatment and prevention groups remained significantly smaller than those of the control group. As expected, tumors in the prevention group were significantly smaller than those of the treatment group over the total 11-week exposure to tazarotene (p<0.05) (Figure 7, inset). In fact, in the prevention group, 6 out of the 10 allografts remained impalpable until week 12, after tazarotene was stopped. We found previously that new autochthonous microscopic BCCs in Ptch1+/− mice did not appear when tazarotene was applied topically for 5 months and then withdrawn for 5 months (So et al 2008). By contrast, when oral tazarotene was stopped the previously non-palpable allograft tumors became palpable within two weeks, and the existing tumors grew larger. The resumed tumor growth was observed for allografts in both treatment and prevention group. When we re-started administration of tazarotene at 2 mg/kg/day in the treatment and prevention groups after a four-week tazarotene “drug-free holiday”, the BCC allografts still responded to tazarotene with a 20–40% tumor volume reduction. These data indicate that oral tazarotene suppresses the growth of BCC allografts but does not eradicate the tumor cells, at least not using the drug administration regimen tested here.

DISCUSSION

Despite technical advances, human BCCs have remained difficult to culture in vitro as established cell lines or to propagate in vivo as xenografts. Here we report a method to generate tumor allografts from ionizing radiation-induced BCCs of Ptch1+/− p53−/− mice, a potent mouse tumor model with essentially defined genetics, and representing the clinical scenario (Aszterbaum et al 1999). In contrast to the previous attempts, the allografts exhibited a dramatically increased engraftment rate and reproduced their parental autochthonous tumors in terms of the histologic and immunophenotypic features as well as response to the anti-BCC effects of tazarotene.

Several differences between our method and those reported in previous studies may be the critical factors underlying our success. First, the nude mice used in most BCC xenograft studies lack functional T cells but have B cells and natural killer (NK) cells; NOD/SCID mice also have complete loss of functional B cells and partial loss of macrophage function and NK cell activity. It has become clear that the immune microenvironment dramatically affects the frequency of tumor uptake. The more severe the immunodeficiency is, the more tolerant the host environment becomes, thus allowing greater rate of tumor formation. In NOD/SCID IL2Rγ^{null} mice, which lack the residual NK cell activity of NOD/SCID mice, even a single melanoma cell can form a tumor (Quintana et al 2008). Secondly, the usage of Matrigel, a reconstituted biologically active basement membrane attachment matrix, may enhance the engraftment rate. Matrigel is comprised of laminin, collagen IV, heparan sulfate proteoglycan and entactin and has been reported to increase the rate of tumor formation and shorten the tumor latency of several tumor types including small-cell lung cancer, renal cell and prostate prostate carcinoma (Fridman et al 1990, Fridman et al 1991, Pretlow et al 1991). Lastly, we used mouse allografts versus the human xenografts. It is well-recognized that xenografts cause more powerful immune responses than allografts as they offer more foreign antigens as targets for an immune response, and the rejection mechanisms are more vigorous in xenogeneic than in allogeneic transplantation.

Our data differ in some respects from those generated by similar studies of allografts of murine medulloblastomas (Sasai et al 2006). Both BCCs and medulloblastomas have higher Gli1 expression in autochthonous tumors than in cell lines established from those tumors but we found downregulation of HH signaling in direct allografts of BCCs. By contrast, direct allografts of medulloblastomas retained their high levels of Gli1 mRNA expression. Furthermore, our cell line expressed increased Gli1 mRNA levels as well as Ptch1 promoter activity (as assessed by β-galactosidase activity) when transferred from in vitro to in vivo conditions; their medulloblastoma cells lines had similar low Gli1 mRNA levels in vitro and in vivo. The above discrepancy may simply be a cancer-type specific phenomenon. In the case of BCCs, our findings highlight the substantial influence of tumor microenvironment on HH activity, which may favor the growth of tumor cells in the ‘new’ host. Therefore, our allograft model offer an excellent system to study the tumor microenvironment, in particular, stromal-tumor cell interactions.

BCC cells are embedded in a dense stroma, which is composed of fibroblasts (cancer associated fibroblasts, CAFs), endothelial cells, inflammatory cells, and abundant

extracellular matrix. Collectively, these components provide a favorable microenvironment to promote survival of cancer cells in both primary and metastatic sites (Liotta and Kohn, 2001). Previous studies reported that the stromal cells surrounding human BCC xenografts contained a mixture of cells from both original tumors (human) and host animal (mouse) (Grimwood et al 1986, Hales et al 1989, Stamp et al 1988). Our data also showed that some, if not all, of the stromal cells in the allografts were from the donor mouse, implying that these stromal cells, probably CAFs, are indispensable for the growth of these allografts.

Tazarotene treated Ptch1+/− mice remained free of visible tumors when tazarotene was discontinued after 5 months of topical treatment (So et al 2008). By contrast, the growth of allografts resumed rapidly once tazarotene was withdrawn. This disprepancy could be due to the fact that the previous experiments studied the effect of tazarotene on microscopic BCCs; however, our allografts were derived from macroscopic tumors, and retinoids are thought to be more effective against early growths. In addition, we used BCCs developed from p53−/− keratinocytes, which are the more aggressive type, in the present study as compared with BCCs arising in p53+/+ mice in the previous experiments. We are in the process of establishing allografts from p53+/+ BCCs and xenografts from human BCCs and evaluating their response to anti-BCC or anti-HH agents.

MATERIALS AND METHODS

Mice

Female NOD/SCID mice were purchased from Jackson laboratory (stock number 001303, Sacramento, CA). Ptch1+/− K14-Cre-ER2 p53fl/fl mice were produced and used to develop BCC tumors [Wang 2011]. All mice were housed under standard conditions (fluorescent lighting 12 hours per day, room temperature 23ºC to 25ºC, and relative humidity 45 to 55%. Animal care and use were in compliance with the protocols approved by the Institutional Animal Care and Use Committee (IACUC) of Children's Hospital Oakland Research Institute (CHORI).

Preparation of tumor cell suspension

Tumors were harvested aseptically from donor mice and briefly incubated in Penicillin:streptomycin (UCSF cell culture facility, San Francisco, CA) with 2 changes of solution. After removing the surrounding skin, the tumors were minced, followed by digestion with 0.25% Trypsin (UCSF cell culture facility), 25U/ml of Dispase (Invitrogen, Carlsbad, CA) or collagenase type I (Invitrogen) at 4ºC overnight. As digestion with collagenase type I generally gave the optimal results, i.e. higher yield and better cell viability, we prepared all tumor cell suspensions with this method for the following experiments. The cell suspensions were diluted with DMEM containing 10% chelexed fetal bovine serum (calcium free) and filtered through 70 μm cell strainers (BD Biosciences, Bedford, MA). After washing twice with DPBS (calcium-free PBS), viable cell counts were determined using 0.4% trypan blue and desired cell concentration were prepared in DPBS.

Injection of tumor cell suspensions and assessment of tumor growth

Tumor cell suspensions were mixed 1:1 with Matrigel (BD Biosciences) and injected subcutaneously into the left and right lateral sides of NOD/SCID mice with 5 mice per group. Tumor growth was monitored weekly, and tumor volume was calculated according to the ellipsoid volume formula ($\pi/6 \times L \times W \times H$).

Immunostaining and quantitative PCR

Tumor fixation, β-Galactosidase staining, Hemotoxylin and eosin (H&E) stain and immunohistochemistry were carried out as described previously [Wang et al 2011]. Briefly, rehydrated samples were subjected to antigen retrieval with rodent decloaker (Biocare Medical, Concord, CA) for 10–20 min at 95–1000C, followed by incubation with rodent block M (Biocare Medical) for 15 min, primary antibody for 1 hr at room temperature or 4C overnight with the following primary antibodies: Ki67 (1:400; Thermo Scientific, Fremont, CA), K14 (1:1000; Covance - Princeton, NJ), collagen IV (1:1000; Abcam, Cambridge, MA), CD31 (1:50; Abcam), Gli1 (1:1000; Rockland, Gilbertsville, PA). Rabbit on rodent HRP-polymer was used as secondary antibody and incubated for 20 min (Biocare Medical). Signal was developed using liquid DAB+ substrate (Dako, Carpinteria, CA) for 2–5 min and counterstained with Cat hematoxylin (Biocare Medical).

For quantitative PCR, total RNA was prepared using either Trizol (Invitrogen) or QuickGene RNA tissue kit SII (Fujifilm, Life Science, Tokyo, Japan) according to the manufacturer's instruction. Quantitative PCR reactions were carried out using the TaqMan Real-time PCR system (Applied Biosystems, Foster City, CA) after reverse transcribing total RNA into cDNA using a high capacity RNA-to-cDNA kit (Applied Biosystems). The TaqMan gene expression assay for Gli1 was purchased (Applied Biosystems).

Fluorescence In situ hybridization (FISH)

FISH was performed with Cy3-conjugated mouse Y chromosome-specific painting probe according to the manufacturer's protocol (Cambio, Cambridge, UK) with the following modifications: 1) pepsin digestion step was replaced with proteinase K (digest-All™ 4, Invitrogen) incubation at room temperature for 1–4 minutes; 2) before mounting with DAPI/antifade solution (Millipore), slides were stained with rabbit polyclonal anti-K14 antibody (1:1000, Covance) followed by incubation with Alexa Fluor 488 conjugated anti-rabbit secondary antibody (1:500, Molecular Probes, Invitrogen). Images were acquired using LSM710 confocal microscope and processed with Zeiss Zen software (Carl Zeiss, Germany).

Systemic administration of Tazarotene

Tazarotene (Allergan, Irvin, CA) was reconstituted in 100% ethanol to yield 100mg/ml stock, which was further diluted with sunflower seed oil (Sigma-Aldrich, St Luis, MO) to get 1mg/ml of working solution. Tazarotene was administered by oral gauvage to mice at 10mg/kg or 2mg/kg with 20-gauge stainless steel, curved feeding needles (New Hyde Park, NY), 5 days per week.

Statistical analyses

The frequency of TIC was determined using L-calc™ software (StemCell Technologies, Inc,). The difference in tumor growth rate between primary tumors and serial transplants (first, secondary and tertiary) was analyzed with week being continuous to model growth rate of change. To assess the effect of tazarotene on allografts, tumor growth was analyzed with a general linear model with repeated measures over time. SAS System (version 9.2) or Microsoft Excel was used for the statistical analysis.

Acknowledgments

We thank Vladimir Serikov for technical assistance on FISH staining; Ginny Gildengorin for statistics; Sam Test and Horst Fischer for helpful support with microscopy; A. Berns for providing p53fl/fl mice; P. Chambon for K14-Cre-ER2 mice; and Yefim Khaimskiy and other members of our lab for invaluable assistance. This study was funded by NIH R01 grant #CA115992.

Abbreviations

BCC	Basal cell carcinoma
HH	hedgehog
Ptch1	Patched
TIC	tumor initiating cell

References

Aszterbaum M, Epstein J, Oro A, Douglas V, LeBoit PE, et al. Ultraviolet and ionizing radiation enhance the growth of BCCs and trichoblastomas in patched heterozygous knockout mice. Nat Med. 1999; 5:1285–91. [PubMed: 10545995]

Carlson JA, Combates NJ, Stenn KS, Prouty SM. Anaplastic neoplasms arising from basal cellcarcinoma xenotransplants into SCID-beige mice. J Cutan Pathol. 2002; 29:268–78. [PubMed: 12100626]

Epstein EH. Basal cell carcinomas: attack of the hedgehog. Nat Rev Cancer. 2008; 8:743–54. [PubMed: 18813320]

Fridman R, Giaccone G, Kanemoto T, Martin GR, Gazdar AF, Mulshine JL. Reconstituted basement membrane (matrigel) and laminin can enhance the tumorigenicity and the drug resistance of small cell lung cancer cell lines. Proc Natl Acad Sci U S A. 1990; 87:6698–702. [PubMed: 2168554]

Fridman R, Kibbey MC, Royce LS, Zain M, Sweeney M, et al. Enhanced tumor growth of both primary and established human and murine tumor cells in athymic mice after coinjection with Matrigel. J Natl Cancer Inst. 1991; 83:769–74. [PubMed: 1789823]

Grimwood RE, Ferris CF, Nielsen LD, Huff JC, Clark RA. Basal cell carcinomas grown in nude mice produce and deposit fibronectin in the extracellular matrix. J Invest Dermatol. 1986; 87:42–6. [PubMed: 3522753]

Grimwood RE, Johnson CA, Ferris CF, Mercill DB, Mellette JR, Huff JC. Transplantation of human basal cell carcinomas to athymic mice. Cancer. 1985; 56:519–23. [PubMed: 3891070]

Grimwood RE, Tharp MD. Growth of human basal cell carcinomas transplanted to C57/Balb/C bgJ/bgJ nu/nu (beige-nude) mice. J Dermatol Surg Oncol. 1991; 17:661–6. [PubMed: 1885829]

Hales SA, Stamp G, Evans M, Fleming KA. Identification of the origin of cells in human basal cell carcinoma xenografts in mice using in situ hybridization. Br J Dermatol. 1989; 120:351–7. [PubMed: 2713256]

Hutchin ME, Kariapper MS, Grachtchouk M, Wang A, Wei L, et al. Sustained Hedgehog signaling is required for basal cell carcinoma proliferation and survival: conditional skin tumorigenesis recapitulates the hair growth cycle. Genes Dev. 2005; 19:214–23. [PubMed: 15625189]

Loning TH, Mackenzie IC. Immunohistochemical studies of basal cell carcinomas transplanted into nude mice. Arch Dermatol Res. 1986; 279:37–43. [PubMed: 2434038]

Mancuso M, Leonardi S, Tanori M, Pasquali E, Pierdomenico M, et al. Hair cycle-dependent basal cell carcinoma tumorigenesis in Ptc1neo67/+ mice exposed to radiation. Cancer Res. 2006; 66:6606–14. [PubMed: 16818633]

Olive KP, Jacobetz MA, Davidson CJ, Gopinathan A, McIntyre D, et al. Inhibition of Hedgehog signaling enhances delivery of chemotherapy in a mouse model of pancreatic cancer. Science. 2009; 324:1457–61. [PubMed: 19460966]

Pawlowski A, Haberman HF. Heterotransplantation of human basal cell carcinomas in “nude” mice. J Invest Dermatol. 1979; 72:310–3. [PubMed: 448164]

Pretlow TG, Delmoro CM, Dilley GG, Spadafora CG, Pretlow TP. Transplantation of human prostatic carcinoma into nude mice in Matrigel. Cancer Res. 1991; 51:3814–7. [PubMed: 2065335]

Quintana E, Shackleton M, Sabel MS, Fullen DR, Johnson TM, Morrison SJ. Efficient tumour formation by single human melanoma cells. Nature. 2008; 456:593–8. [PubMed: 19052619]

Sasai K, Romer JT, Lee Y, Finkelstein D, Fuller C, et al. Shh pathway activity is down-regulated in cultured medulloblastoma cells: implications for preclinical studies. Cancer Res. 2006; 66:4215–22. [PubMed: 16618744]

So PL, Fujimoto MA, Epstein EH Jr. Pharmacologic retinoid signaling and physiologic retinoic acid receptor signaling inhibit basal cell carcinoma tumorigenesis. Mol Cancer Ther. 2008; 7:1275–84. [PubMed: 18483315]

So PL, Langston AW, Daniallinia N, Hebert JL, Fujimoto MA, et al. Long-term establishment, characterization and manipulation of cell lines from mouse basal cell carcinoma tumors. Exp Dermatol. 2006; 15:742–50. [PubMed: 16881970]

So PL, Lee K, Hebert J, Walker P, Lu Y, et al. Topical tazarotene chemoprevention reduces Basal cell carcinoma number and size in Ptch1+/− mice exposed to ultraviolet or ionizing radiation. Cancer Res. 2004; 64:4385–9. [PubMed: 15231643]

Stamp GW, Quaba A, Braithwaite A, Wright NA. Basal cell carcinoma xenografts in nude mice: studies on epithelial differentiation and stromal relationships. J Pathol. 1988; 156:213–25. [PubMed: 3204452]

Wang GY, Wang J, Mancianti ML, Epstein EH Jr. Basal cell carcinomas arise from hair follicle stem cells in ptch1(+/−) mice. Cancer Cell. 2011; 19:114–24. [PubMed: 21215705]

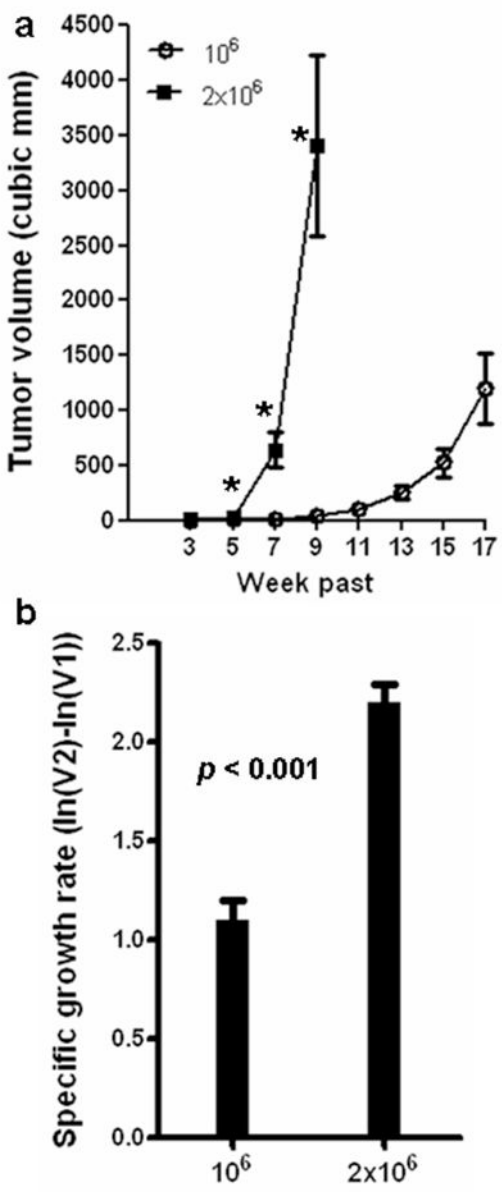

Figure 1.

The growth rate of the allografts was dose-dependent. (a) The tumor volumes were significantly different between the 2 doses for week 5 (3.7±2.5 vs. 30.59±8.4, $p<0.05$), week 7 and week 9 ($p<0.05$, noted with *). According to the mouse protocol, all the mice that were injected with 2×10^6 cells were euthanized at week 9 due to over-sized tumors. (b) The specific growth rate [calculated by ln(V2) - ln(V1)] of the allografts injected with 2×10^6 cells was significantly higher than those injected with 10^6 cells. Data shown are average ± SEM, n=6 for each group.

a

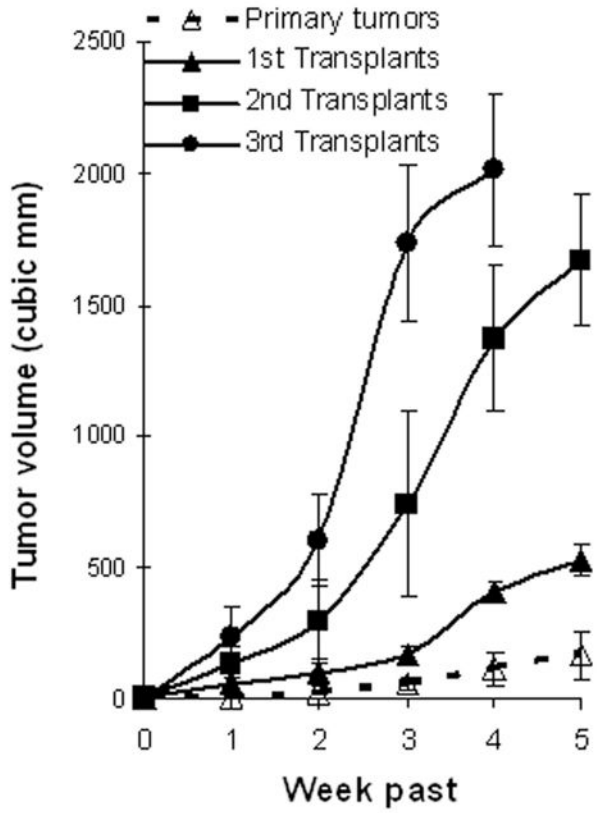

b

Serial transplants	1st	2nd	3rd
Primary	<0.001	<0.0001	<0.0001
1st transplant		<0.01	<0.0001
2nd transplant			<0.05

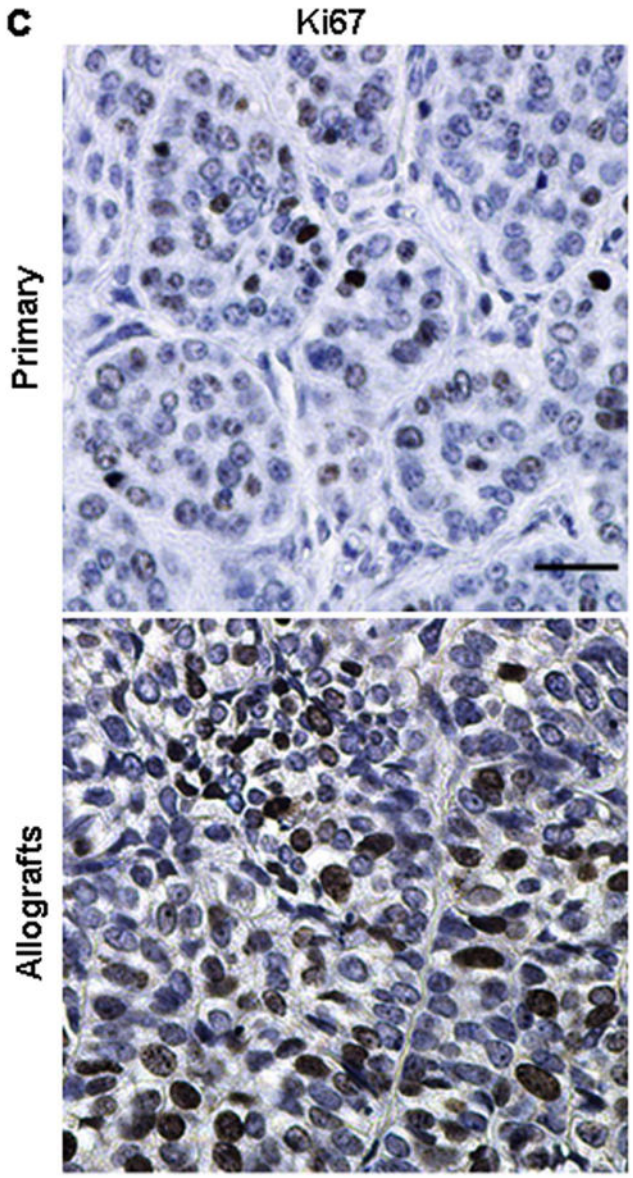

Figure 2.

Tumor growth rate increased through serial in vivo passaging. (a) The tumor volumes were plotted against the week past since the appearance of the first palpable tumor (defined as week 0). Data shown are average ± SEM, n=5 for each group. (b) p values of TTEST between groups are shown. (c) Representative images show that there were more Ki67-positive cells in allografts than the primary tumors. Scale bars=20μm.

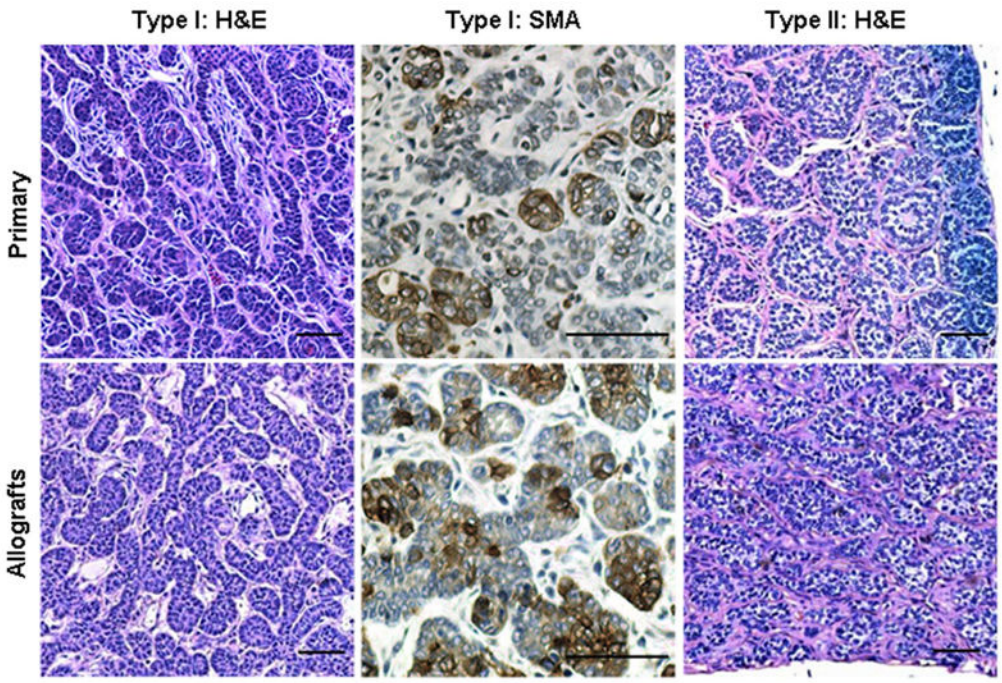

Figure 3.

The allografts inherited the histopathologic features of their original tumors. The allografts and their parental tumors were stained with H&E or anti-SMA antibody and assessed for type I (characterized by branching and radiating tumor cells, SMA-positive) or type II (characterized by basaloid cells arrayed in nests, SMA-negative) classification. Four primary tumors (2 for each type) and the allografts derived from them (n=4 for each primary tumor) were analyzed. Scale bars=50μm.

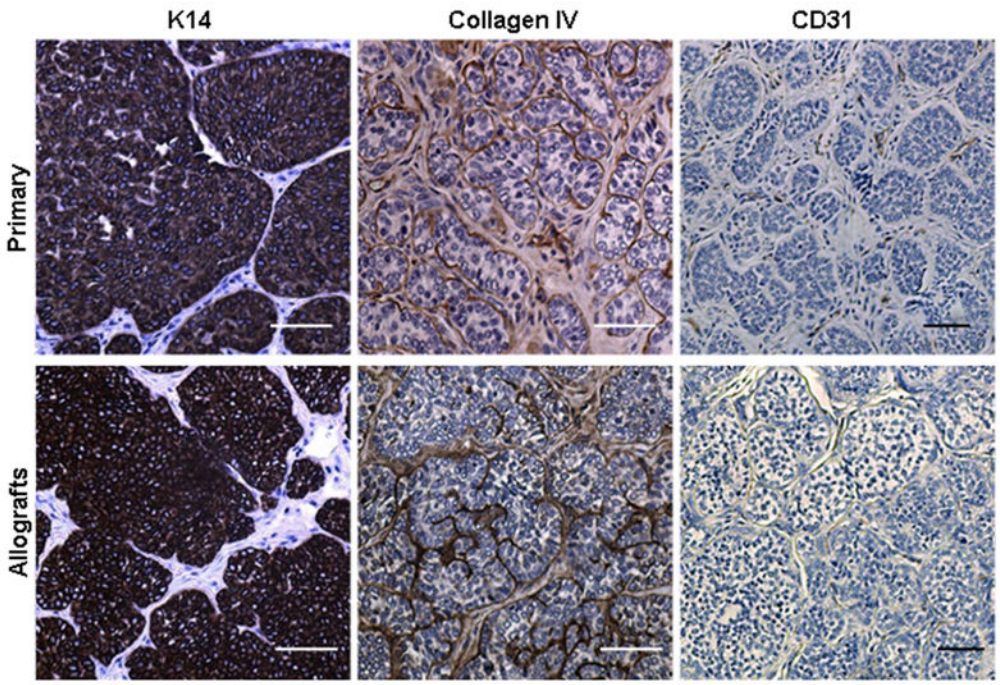

Figure 4.

The allografts reproduced the Immunophenotypic features of their original tumors. The allografts and their parental tumors were stained with anti-K14, anti-collagen IV and anti-CD31 antibodies to assess the basal keratinocyte cell of origin, stroma density and vasculature properties. Scale bars=50μm.

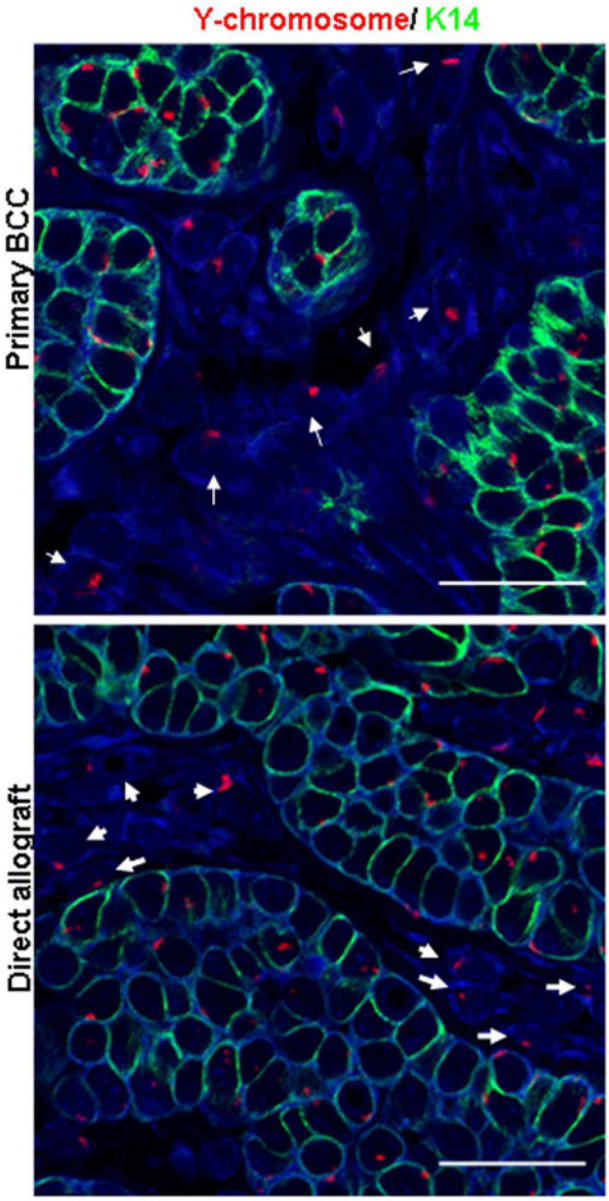

Figure 5.

The stromal cells from the original mouse were detected in direct allografts. Primary BCCs generated from male mouse were injected into female NODSCID mice. FISH was performed to detect cells from male donor mice with Cy3-conjugated Y chromosome-specific painting probe (red). BCC tumor cells were stained with keratin 14 antibody (green). Y chromosome-positive and K14-negative stromal cells were identified (arrows). Scale bars=20μm.

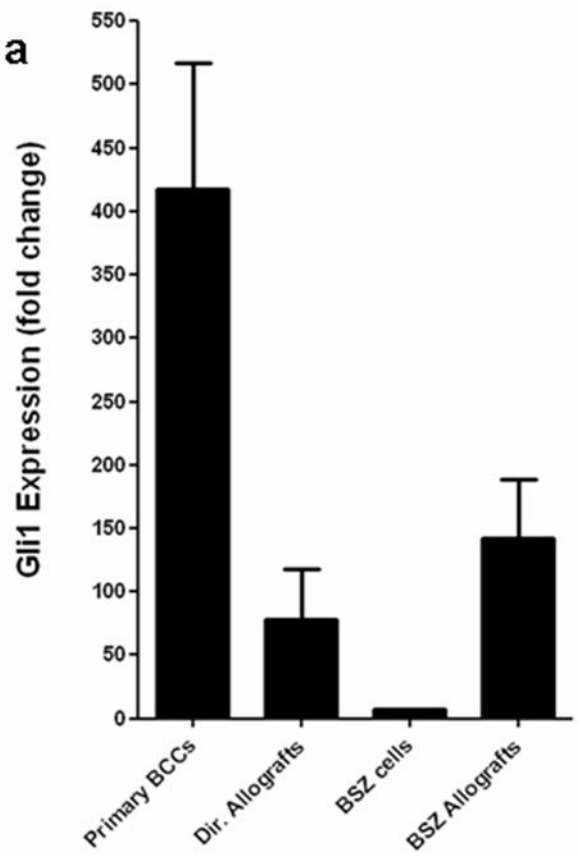

b

	Direct allografts	BSZ cells	BSZ allografts
Primary BCCs	0.006	0.001	0.022
Direct allografts		0.111	0.314
BSZ cells			0.020

Figure 6.

Hedgehog signaling activity. (a) Gene expression level of Gli1 was determined by quantitative PCR for primary BCCs (n=14), direct allografts (n=9), BSZ cells (n=3), and BSZ allografts (n=9). Y-axis: fold changes (normalized by β-actin endogenous control) for each assay. Identical thresholds of 0.2 were set for all runs with four technical replicates. Data shown are average ± SEM. (b) p values of statistical analysis between groups by TTEST.

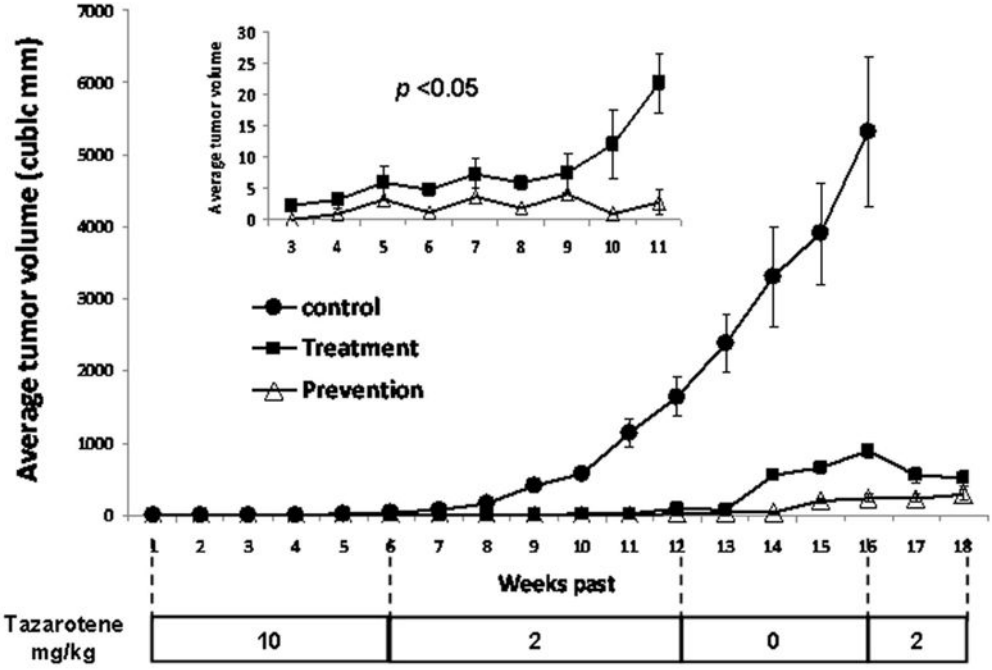

Figure 7.

BCC allografts responded to tazarotene treatment. The allografts were randomly divided into 3 groups: the prevention group (n=10) received tazarotene when tumor cells were injected (defined as week 0); treatment group (n=10) received tazatotene once palpable tumors were observed (i.e. week 3); and the control group (n=8) received no treatment. Tumor volumes (measured once a week) are plotted against week past. Inset: prevention and treatment groups are plotted with a small scale of Y-axis for tazarotene exposure period of week 3 to week 11. It appeared that the treatment group grew significantly faster than the prevention (TTEST, paired, $p<0.05$). Data shown are average ± SEM.